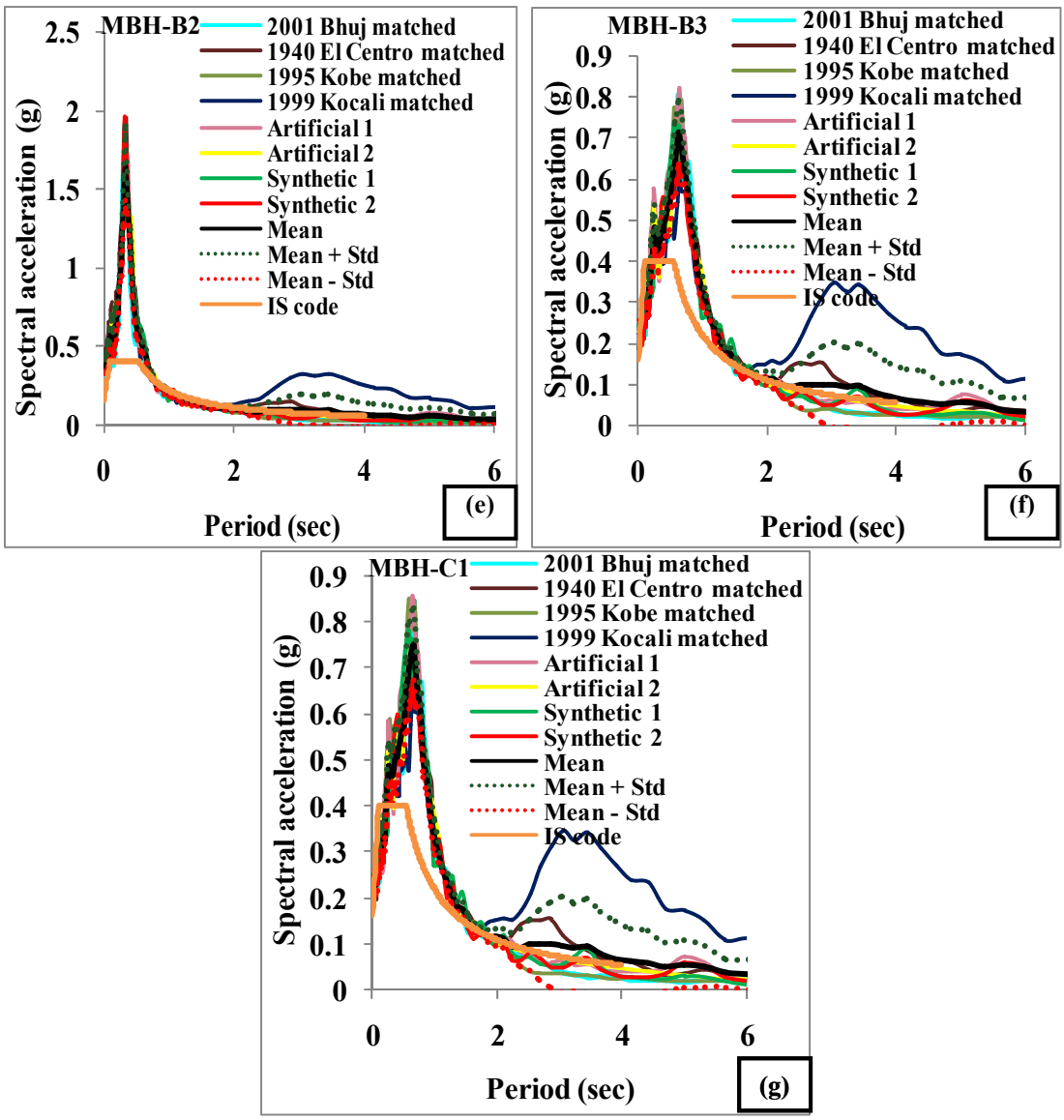

FIG. 7. Response spectrum obtained by GRA for the boreholes (a) MBH-A2, (b) MBH-A3, (c) MBH-A4, (d) MBH-B1, (e) MBH-B2, (f) MBH-B3 and (g) MBH-C1.

The surface time histories obtained from SGRA using *DEEPSOIL v6.0* software (Hashash et al., 2014) were further analyzed to find out the ground motion parameters at the surface. Ground motion parameters at the surface for the generated time histories by considering Indian seismic codal spectrum (IS code spectrum) were analyzed using *SeismoSignal 2.1.0* software. The ground motion parameters at the surface for the generated time histories for the boreholes LBH-1 and MBH-A1 are presented in Table 3. Similar analysis was done for all the remaining borehole locations at the port site. The influence of the local soils in modifying the characteristics of the bedrock motion is distinctively seen in the ground motion parameters. In the work carried out by Naik (2015), other sites located in the same

city as that of the port, having pre-dominantly silty soils were found to be amplifying type with an amplification factor between 6 to 7.

Table 3. Ground motion parameters at the surface for generated time histories.

BH	Parameter	Time history							
		2001 Bhuj	1940 El Centro	1999 Kobe	1995 Kocaeli	Art 1	Art 2	Syn 1	Syn 2
LBH-1	Max. Acceleration (g)	0.29	0.29	0.26	0.28	0.28	0.26	0.3	0.28
	Sustained Maximum acceleration (g)	0.19	0.24	0.24	0.26	0.22	0.24	0.18	0.26
	Effective design acceleration (g)	0.29	0.29	0.26	0.27	0.28	0.25	0.3	0.28
	Predominant Period (sec)	0.52	0.54	0.52	0.52	0.54	0.54	0.54	0.54
	Mean Period (sec)	0.59	0.57	0.56	0.97	0.58	0.58	0.58	0.57
	Bracketed Duration (sec)	66.2	30.46	37.7	28.16	19.8	21.1	7.26	7.3
MBH-A1	Max. Acceleration (g)	0.3	0.39	0.34	0.34	0.33	0.32	0.32	0.32
	Sustained Maximum acceleration (g)	0.23	0.31	0.31	0.3	0.25	0.27	0.23	0.24
	Effective design acceleration (g)	0.3	0.4	0.34	0.34	0.33	0.32	0.33	0.32
	Predominant Period (sec)	0.44	0.46	0.46	0.46	0.46	0.44	0.46	0.52
	Mean Period (sec)	0.5	0.47	0.47	0.83	0.52	0.49	0.49	0.5
	Bracketed Duration (sec)	54.9	29.6	35.6	26.28	19.7	20.6	7.26	7.3

CONCLUSIONS

Seismic ground response analysis was carried out for the Mormugao port in Goa, India. The analysis was conducted on nine boreholes using 8 input motions selected based on three criteria's of selection. The input motions were matched with the Indian seismic codal spectrum. The conclusions of the study can be briefly stated as follows:
1) Earthquake time histories were obtained by matching actual earthquake time histories with Indian seismic codal spectrum for zone III and rock sites, artificial and synthetic earthquakes were also generated. A suite of 8 input motions matching the codal spectrum were developed. The generated time histories were analyzed and ground motion parameters at the bedrock were evaluated using *SeismoSignal 2.1.0*. The predominant period at the bedrock was observed to vary from 0.02 to 0.3 sec and the maximum horizontal acceleration varied from 0.018 to 0.346 g.
2) SGRA was carried out for the nine locations using *DEEPSOIL v6.0* software. The response spectrum obtained from GRA was compared with the response spectrum given by Indian seismic code IS1893 (Part1): 2002 for soft soil sites. It was seen that higher spectral accelerations were obtained as compared to IS code spectrum. The GRA considering IS code spectrum gave maximum amplification ratio (considering Fourier amplitude) of 12.69. Based on the study, it was observed that time histories with higher duration gives more amplification as compared with time histories with lower duration.

3) Ground shaking is stronger where shear wave velocity is lower as the soil stiffness is directly related to the shear wave velocity. It was also observed that soft soils amplify more. It has been observed that borehole MBH-A3 gives maximum amplification among all the boreholes.
4) Time period plays a very important role in the seismic ground response analysis. Depending upon the input motion period and the individual soil layer period, amplification and de-amplification was observed, as can be noted in the plot of variation of PGA with depth.

ACKNOWLEDGMENT

The authors would like to thank the Mormugao Port Trust (MPT), Goa for providing the borehole data from the port site.

REFERENCES

Bilham, R. and Gaur, V. K. (2011). " Historical and future seismicity near Jaitapur, India." *Current Science,* Vol.101: 1275-1281.

Desai, S.S. and Choudhury, D. (2014a). "Spatial variation of probabilistic seismic hazard for Mumbai and surrounding region." *Natural Hazards*, Vol. 71(3):1873–1898.

Desai, S.S. and Choudhury, D. (2014b). "Deaggregation of seismic hazard for two ports in Mumbai metropolitan region." in International conference on geotechnical engineering, *GeoShanghai 2014: Advances in Soil Dynamics and Foundation Engineering, GSP 240*, ASCE, 62–71.

Hashash, Y.M.A, Groholski, D.R., Phillips, C. A., Park, D. and Musgrove, M. (2014) *DEEPSOIL v6.0*, User Manual and Tutorial.,107 p.

IS1893 (2002). "Criteria for earthquake resistant design of structure." *Bureau of Indian Standards*, New Delhi, Part I.

Mhaske, S. and Choudhury, D. (2011). "Geospatial contour mapping of shear wave velocity for Mumbai city." *Natural Hazards,* Vol. Vol. 59: 317 – 327.

Naik, N. P.(2015). "Site specific seismic hazard studies for the state of Goa." *Ph.D thesis*, IIT Bombay.

Naik, N.P. and Choudhury, D. (2014). "Development of Fault and Seismicity Maps for the State of Goa, India." *Disaster Advances,* Vol. 7(6):12-24.

NEHRP, (National Earthquake Hazard Reduction Program) (2009), Recommended provisions for seismic regulations for new buildings and other structures – Part 1: Provisions, Prepared by the Building Seismic Safety Council for the Federal Emergency Mangement Agency (Report FEMA 450), Washington DC.

Raghukanth, S. T. G. and Iyengar, R. N. (2006). "Seismic hazard estimation for Mumbai city." *Current Science,* Vol. 91(11):1486.

SeismoArtif version 2.1.0, www.seismosoft.com.

SeismoMatch version 2.1.0, www.seismosoft.com.

SeismoSignal version 2.1.0, www.seismosoft.com.

Xia, J., Miller, R. D., Park, C. B. (1999). "Estimation of near-surface shear-wave velocity by inversion of Rayleigh waves." *Geophysics*, Vol. 64(3): 691-700.

A Case Study of the Impact of Tropical Storms on the Stability of Natural Hillslopes in Macon County, North Carolina

Giuseppe Formetta[1]; Alexandra Wayllace[2]; and Ning Lu, F.ASCE[3]

[1]Postdoctoral, Dept. of Civil and Environmental Engineering, Colorado School of Mines, Golden, CO 80401. E-mail: formetta@mines.edu
[2]Teaching Associate Professor, Dept. of Civil and Environmental Engineering, Colorado School of Mines, Golden, CO 80401. E-mail: awayllac@mines.edu
[3]Professor, F.ASCE, Dept. of Civil and Environmental Engineering, Colorado School of Mines, Golden, CO 80401. E-mail: ninglu@mines.edu

Abstract: Rainfall-induced shallow landslides are one of the most significant hazards in mountain areas. In order to analyze and eventually predict the timing and locations of landslides triggering, we use a recent established USGS Hillslope FS2 model to simulate the hillslope hydrology and stability. Stresses, soil moisture, and soil suction are concurrently simulated by a coupled variably saturated flow and stress fields finite element model. The hydro-mechanical framework is applied to a hillslope in Macon County, North Carolina. Here, extensive failure of hillslopes often occurs after heavy tropical storms. In recent years, we conducted site monitoring of soil moisture and suction at different depths in some landslide-prone hillslopes. The objectives of the case study were: i) to simulate the stability conditions of the monitored slopes during hurricanes Frances and Ivan and ii) to identify a possible rainfall scenario for slope failure. The application involved the calibration of the hillslope hydro-mechanical properties by using the measured soil moisture and suction data. Results show that the hillslope was stable under the rainfall of hurricanes Frances and Ivan. However, it would fail if the intensity of the rainfall increased by a factor of 1.3.

INTRODUCTION

Precipitation-induced landslides are one of the most serious environmental hazards and constitute a serious threat to public safety. In subtropical climatic regions, with mountainous topography, rainfall is generally the most common cause of landslides. Geo-environmental factors such as geology, land-use, vegetation, climate, increasing population may increase the landslides occurrence (Sidle and Ochiai 2006).

To improve the predictability of shallow landslides, many authors (Montgomery and Dietrich 1994; Baum et al. 2008) developed physically based slope-stability models that synthetizes the interaction between hydrology, geomorphology, and soil

mechanics (Lu and Godt, 2013). In general, they include a hydrological component to simulate infiltration and groundwater flow processes and a soil-stability component to simulate the safety factor of the slope. Several models are available in literature with different degrees of complexity. Typical hydrological components range from steady state (Montgomery and Dietrich, 1994) to transient groundwater flow (Simoni et al., 2008). Common slope stability components are based on limit-equilibrium methods (Fellenius, 1936; Janbu, 1973) or shear strength reduction analysis (Smith and Griffiths, 2004). Recently the framework proposed by Lu et al., 2012 allows to compute a scalar field of factor of safety defined for each point of the hillslope differently from limit-equilibrium method that defines a single stability indicator for the entire hillslope.

Western North Carolina (Fig. 1) is an area particularly exposed to heavy-rainfall induced landslides especially because of the concentration of orographic precipitations and hurricanes, the presence of steep slopes and thin soil depths (Witt, 2005). Landslides in this area are triggered by subtropical storm systems (Wooten et al., 2008) and are predominantly influenced by antecedent soil moisture condition. One recent example is Hurricanes Frances and Ivan, which caused 5 deaths, and destroyed 27 homes.

In this paper we conducted a 2D slope stability analysis of a hillslope located in Western North Carolina (Fig. 1) under the Hurricanes Frances and Ivan. We used the recently established USGS Hillslope FS2 model to simulate the hillslope hydrology and stability based on the framework presented in Lu et al. (2012). The model computes soil moisture and soil suction fields solving the 2D Richards equation and soil total stress solving the 2D linear elasticity equation. Finally, effective stress and local factor of safety are computed based on the suctions stress theory (Lu and Likos, 2004).

The model application involves three steps. First, to identify the hillslope hydro-mechanical properties we calibrated the model parameters using on site measurements of pressure head and soil moisture at three different depths (0.4, 0.9, and 1.35 m). Then we performed the hillslope stability analysis using the rainfall measured during the hurricanes Frances and Ivan. Finally, to establish which rainfall scenario would cause instability, we iteratively increased the rainfall intensity until the hillslope fails.

STUDY AREA

The case study Mooney-Gap (Fig. 1) is located in the Southern Appalachian Mountains of Macon County, North Carolina (southeastern USA). The Macon County (Wooten et al. 2008), has an extension of 1350 km^2, and elevation ranges between 500 and 1650 m. Average annual precipitation varies between 1800 and 2400 mm and average annual air temperature ranges from 11 to 14 °C. In September 2004, this area was damaged by heavy rainfall from the remnants of the Hurricanes Frances (September, 7-8) and Ivan (September, 16-17). These events caused catastrophic consequences: 155 triggered landslides, 5 deaths, 27 homes destroyed (Wooten et al 2008).

The monitoring site was located in a hill that did not fail during the Hurricanes Frances and Ivan. A monitoring system was installed on the hillslope in order to

collect hourly measurements of rainfall, and soil suction and soil water content at three different depths (0.4, 0.9 and 1.35 m). The collected data covers a two months period, from 01-11-2014 to 01-01-2015. The altimetric profile of the two analyzed hillslopes (Fig. 1 - black triangle and black circle) was extracted from a 6 meters resolution LIDAR digital elevation model provided by North Carolina Department of Transportation. The geological profile reported in Fig. 1 was drawn on the basis of on site stratigraphy measurements.

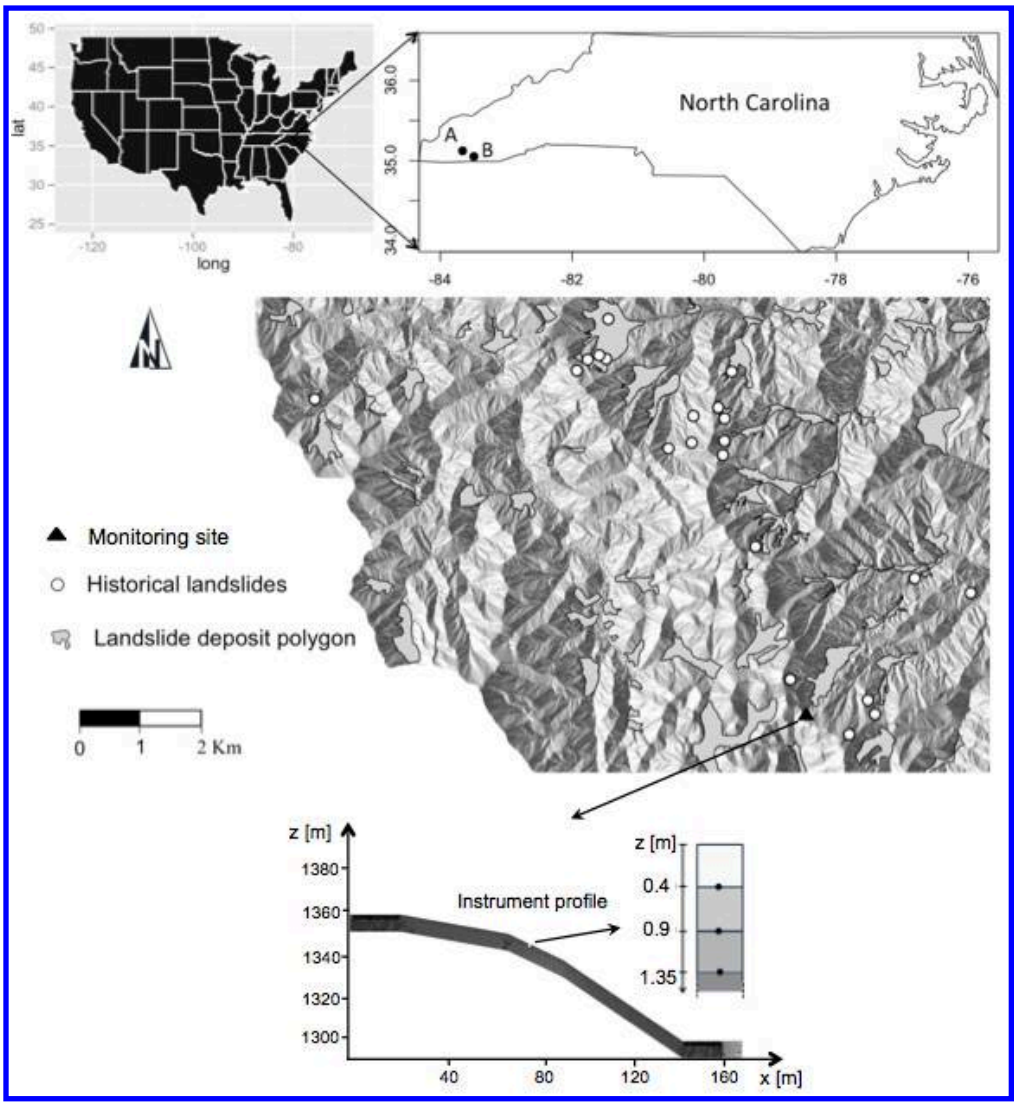

FIG. 1. Mooney-Gap study area localization: historical landslides and monitored site.

HYDRO-MECHANICAL FRAMEWORK

The stability analysis of the monitored hillslope was carried out according the framework presented in Lu et al., 2012. It involves the computation of soil moisture,

soil suction, and gravity induced soil total stress fields. The use of the suction stress theory allows the computation of the effective stress ensuring a mathematically consistent description of transition between saturated-unsaturated states. Finally, the potential unstable areas are detected using the field of local factor of safety (Lu et al., 2012) that is capable of capturing the shifting of stress paths toward the failure state due to transient rainfall infiltration.

The model implements one way coupling of two existing finite element codes. The first is based on FEM2D (Reddy, 1985) and solves the governing equations for plain strain linear elasticity. The second program is based on the hydrological model SWMS-2D (Simunek et al., 1994) which solves Richards equation for unsaturated flow.

Estimation of the on site Van Genuchten and Mualem parameters was performed using the automatic model parameters optimization (MPO) integrated in the software HYDRUS-2D. This optimization implements the Levenberg-Marquardt optimization algorithm in order to find the parameter set that minimizes the difference between modeled and observed data.

RESULTS

The MPO-HYDRUS component was used to estimate the model parameter set that minimizes the differences between observed and simulated values of soil moisture and soil suction. The model initial conditions were computed using an infiltration process with a low rainfall rate (0.0001 m/h) until the soil water content and soil suction dynamic reached a stationary state close to the initial measured values. No flow boundary conditions were set at the bottom and at the upper-left side of the hillslope. Seepage boundary conditions were set at the lower-right side of the hillslope and this was justified by the presence of a creek. Atmospheric boundary conditions were applied at the top of the hillslope.

The optimization process was carried out at the three locations (0.4, 0.90, and 1.35 m depth). We split the two months soil moisture and pressure head measured data in half and we used one month for model parameter calibration and one month for model simulation. The estimated optimal parameter set is presented in Table 1 where θr is the residual water content, θs is the saturated water content, α and n are Van Genuchten parameters, and ks is the saturated hydraulic conductivity. Parameter values determined by using the inverse modeling procedure have typical values of the soil in site classified as silty sands and silty clays (Lewis et al., 2013). Figure 2 presents the comparison between modeled and measured soil moisture and pressure head at the three different depths. The model is able to mimic the dynamic behavior of both soil moisture and soil suction in the three sensor locations (at 0.40, 0.9, and 1.35 m depth) both in calibration and simulation periods. For this reason we used the estimated optimal parameter set to carry out the stability analysis.

Table 1. Optimal parameters estimated for each soil layer.

	θ_r [-]	θ_s [-]	α [1/m]	n [-]	k_s [m/h]
Layer 1	0.24	0.40	4.0	1.70	0.10
Layer 2	0.26	0.42	4.2	1.55	0.12
Layer 3	0.23	0.45	4.3	1.85	0.04

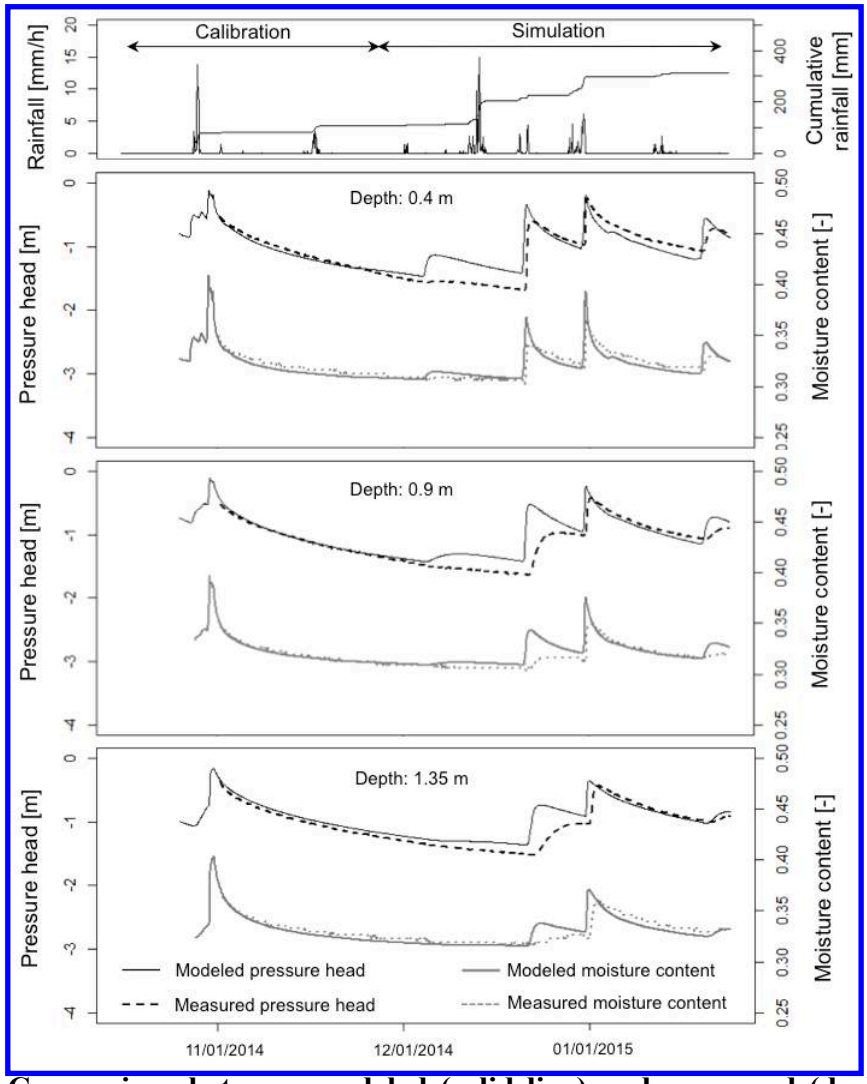

FIG. 2. Comparison between modeled (solid line) and measured (dashed line) moisture content (in gray) and pressure head (in black). Results are provided at the three different depths: 0.4, 0.9, and 1.35 m.

Boundary conditions for the mechanical model were rollers at the hillslope bottom and sides. Therefore vertical displacement is zero at the base and horizontal displacement is zero at the sides. Mechanical properties used for the stability analysis are presented in Table 2 where c' is effective cohesion, ϕ' is the effective friction angle, E is the Young modulus, μ is the Poisson's ratio, and γ is the dry unit weight of the soil.

The rainfall that occurred during hurricanes Frances and Ivan was measured in the Mooney Gap station (RG31 at 1364 m) and was used as input of the hydro-mechanical framework in order to simulate the stability conditions of the hillslope. Moreover, in order to define the rainfall scenario that would cause failure, we iteratively increased the measured rainfall that occurred during Hurricanes Frances and Ivan stopping the analysis when the safety factor decreased to less than 1.0. We found that increasing the rainfall occurred during hurricanes Frances and Ivan by 30% would cause the hillslope failure. Suction stress and field of local factor of safety are reported in Fig. 3 for the measured Frances and Ivan rainfall, and in Fig. 4 for the 30% increased rainfall.

Table 2. Parameters used for the mechanical model.

	c' [kPa]	ϕ' [°]	E [MPa]	μ [-]	γ [kN/m^3]
Layer 1	15	38	10.0	0.33	16.0
Layer 2	12	40	10.0	0.33	16.0
Layer 3	12	40	10.0	0.33	16.0

Results are presented at three different times: before the hurricanes, after the peak of hurricane Frances, and after the peak of hurricane Ivan. Figures 3 and 4 show that during the hurricanes Frances and Ivan suction stress decreases mainly near the soil surface up to 1.5 m in depth. Suction stress near the crest and the toe of the hillslope decreases to values between 1-2 kPa for the measured Frances and Ivan rainfall and to values between 0-1 kPa for scenario with 30% increased rainfall.. Fig. 3 shows that the hillslope was stable during hurricanes Frances and Ivan. Local factor of safety decreases in the top-soil due to the infiltration process and corresponding decreasing of suction stress. Fig. 4 shows the failure evolution of the hillslope for the 30% increased rainfall scenario. In black is depicted the area with local factor of safety lower than 1 and a black line delineates the surface of failure. The failure surface depth is about 0.8 m which is consistent with observations of landslides that occurred during Frances and Ivan in the area (Wooten et al. 2008). A small area presenting safety factor lower than 1 is observed in the upper gentle slope section of the hillslope. This is probably due to a combination of being close to a boundary and having a sudden change in slope.

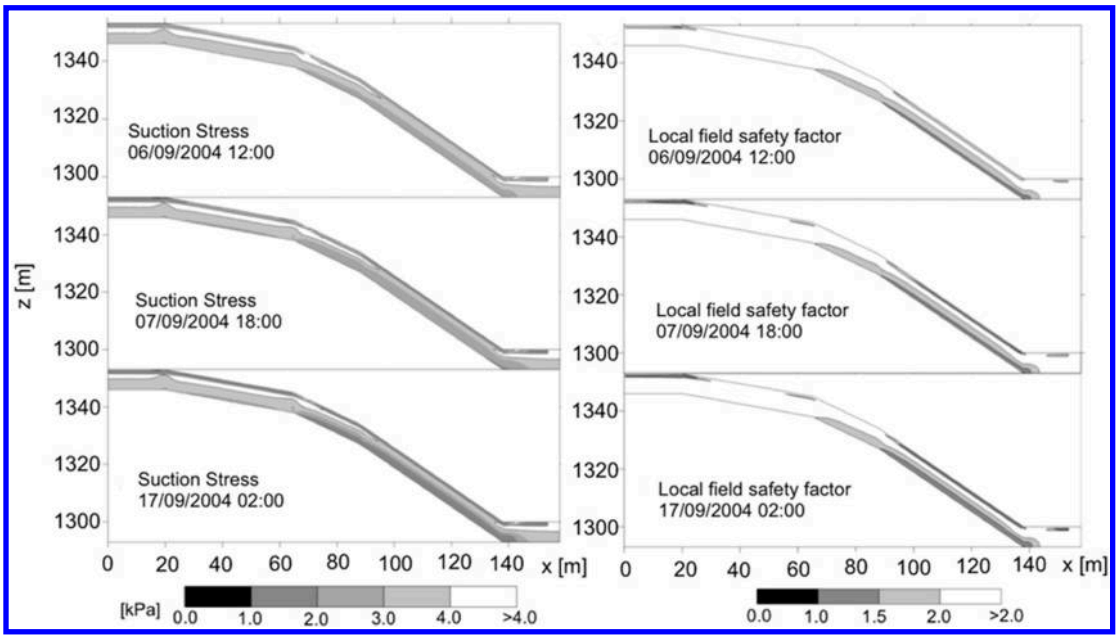

FIG. 3. Suction stress and local factor of safety during the Frances and Ivan rainfall at three different times: before the hurricanes, after the Frances peak, and after the Ivan peak.

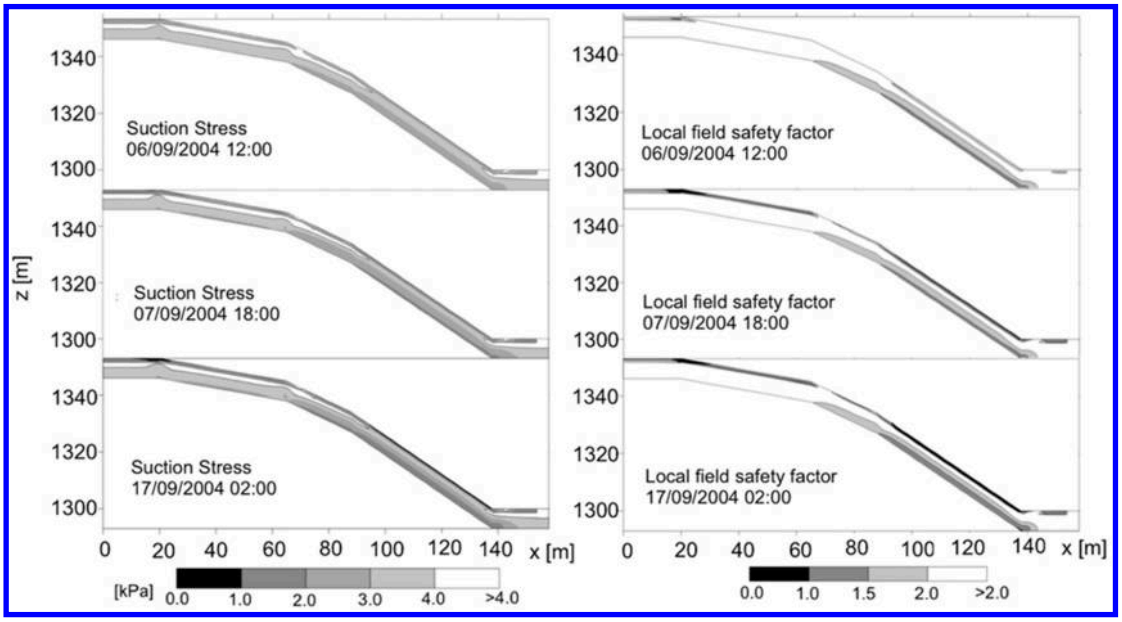

FIG. 4. Suction stress and local factor of safety during the 30% increased Frances and Ivan rainfall at three different times: before the hurricanes, after the Frances peak, and after the Ivan peak.